Hindawi
Shock and Vibration
Volume 2021, Article ID 7403365, 11 pages
https://doi.org/10.1155/2021/7403365

Research Article

Numerical Study on the Mechanical Properties of Transmission Tower K-Joints under Cyclic Loading

Jia-xiang Li, Chao Zhang, Shu-hong Wang, and Sheng-qiang Yin

Department of Civil Engineering, Northeastern University, Shenyang, Liaoning Province, China

Correspondence should be addressed to Chao Zhang; zhangchao_neu@126.com

Received 20 September 2021; Accepted 21 October 2021; Published 8 November 2021

Academic Editor: Bing Qu

During the vibration of a transmission tower, the joints will be subjected to a reciprocating load. To obtain the accurate state of the transmission tower under the load, the mechanical properties of the joints under the vibration load must be considered. In this paper, the mechanical properties of typical K-joints in transmission tower structures are studied by numerical simulation. The failure mode of the K-joint under cyclic loading is also analyzed. The mechanical properties of the K-joint are discussed from the aspects of hysteretic characteristics, stiffness degradation, energy dissipation capacity, and ductility evaluation, and the influencing factors are discussed. The results show that the failure mode of the K-joint is related to the bolt grade and steel strength. When analyzing K-joints, the moment-rotation hysteresis curve should be combined with the realistic parameters of joints to consider the hysteretic behavior of the K-joint. The results provide a theoretical reference for the accurate modeling of transmission towers.

1. Introduction

Joints are the connecting parts between structural components. The mechanical characteristics of joints have a significant impact on the entire structure. In traditional analysis methods, joints are often assumed to be hinged or rigid. In fact, the mechanical characteristics of joints are between ideal hinged joints and complete rigid joints. They have a certain rotational stiffness and can bear part of the bending moment when a certain rotation occurs. To obtain the true mechanical response of structures, semirigid joints must be considered [1–3]. At present, research on semirigid joints mostly focuses on the beam-column connections of frame structures. Zhu et al. [4] obtained the moment-rotation curve of the bolted end plate in the range of elasticity, plasticity, ultimate, and fracture by experiment, gave the failure mechanism of the structural components, and compared it with AISC design guide and European standard. The results showed that both methods underestimate the ultimate moment of joints. Based on the two-parameter exponential model, Zhou et al. [5] proposed a practical analysis model of the moment-rotation relation, which can predict the ultimate flexural capacity of steel beams to concrete-filled steel tube column connections with bidirectional bolts with different size parameters and material properties. Faridmehr et al. [6] carried out cyclic loading tests on rigid and semirigid steel beam-column connections. The results show that the rigid connection has a greater energy dissipation capacity and equivalent hysteretic damping ratio under a larger interstory drift angle. However, lattice structures such as towers and grids are composed of structural steel, steel pipes, or composite section bars, and semirigid joints are completely different from beam-column joints. According to the connection mode, joints can be roughly divided into bolt and welded joints. During installation, the steel pipe is often welded, and some areas are connected with bolts. Shao et al. [7] and Dodaran et al. [8] studied the structural performance of tubular K-joints at high temperature, and the results showed that the ultimate strength of the joints would decrease with increasing temperature. Feng et al. [9, 10] studied the effect of different parameters on the failure mode and bearing capacity of stainless steel tubular K-joints through experimental and numerical methods and proposed a formula to accurately predict the ultimate stress of tubular K-joints.

Due to frequent maritime accidents, the offshore platform will accidentally collide. Therefore, Lu et al. [11] studied the mechanical characteristics of tubular K-joints of offshore platforms under impact loading by experiments and simulations. The results show that in numerical simulation, it is essential to accurately define the dynamic characteristics of materials for predicting the impact response of the K-joint. In addition to the grid structure, tubular steel towers are also basically composed of welded structures and have the characteristics of lightweight and good mechanical characteristics. Li et al. [12, 13] studied the bearing capacity of tubular K-joints with 1/2 or 1/4 annular plates by full-scale experiments. The results indicated that annular plates can improve the bearing capacity of the joints. The angle steel is mostly connected by bolts. For convenient installation, there is a structural clearance of approximately 1.5 mm–4.0 mm between the bolt shank and hole, which causes relative sliding between structural members, also known as bolt slippage. The sliding distance depends on the relative position of the bolt shank in the bolt hole and clearance size. Jiang et al. [14, 15] studied joint slip by experiments and numerical simulations. The results show that bolt slip not only affects the displacement of the transmission tower but also affects the ultimate bearing capacity and failure mode of the transmission tower. Yang et al. [16] and An et al. [17] studied the influence of different parameters on the load-deformation curve of bolted joints through tensile tests and finite element simulations of transmission tower bolt joints. The results showed that when analyzing the transmission tower structure, if the joint slip effect was ignored, the axial stiffness of the joints would be significantly overestimated. To accurately predict the tower deflection, Gan et al. [18] proposed a joint-slippage model based on the component method to predict the tower deflection. For K-joints, Zhao et al. [19] used the component method to derive the calculation model of the initial rotational stiffness of the angle steel tower K-joints and corrected it by combining five full-scale tests. It was verified that the number of bolts and bolt spacing were important factors affecting the initial stiffness of such joints. Yang et al. [20] improved the traditional unit load method by studying the K-joint of the crank arms of UHV cat-head transmission towers.

However, the above studies are all for the static calculation of transmission towers, which are not suitable for dynamic calculation. As a high-rise structure, the transmission tower will be subjected to severe wind, ice shedding, earthquakes, and other loads during service, which will cause the vibration of the transmission tower, threaten the normal operation of the transmission tower, and even lead to the collapse of the transmission tower [21]. During the vibration of the transmission tower, joints will be subjected to cyclic loading. Previous studies have shown that the failure mode, ultimate bearing capacity, and ultimate deformation capacity of steel structure joints are different under both monotonic and cyclic loading [22]. In the vibration process of a transmission tower, the loading state (size and direction) of joints will change, and the model obtained by the monotonic loading test cannot well reflect the mechanical characteristics of the joint in the dynamic process. Therefore, it is necessary to study the cyclic loading of typical transmission tower joints to determine the mechanical characteristics in the vibration process. Li et al. [23] analyzed the hysteretic performance of transmission tower typical bolt joints under cyclic loading and studied the effects of bolt slip on the hysteresis performance joints. The results showed that the hysteretic effect of bolt slip should be considered when calculating the dynamic response of the transmission tower. Ma et al. [24] proposed a hysteretic model of single-bolted angle joints considering cyclic bolt slip, which can more effectively study the joint behavior of towers.

A review of the abovementioned works indicates that the mechanical characteristics of K-bolt joints under cyclic loading should be studied. In this paper, the K-joint of a 500 kV transmission tower is employed as the research object, and the hysteresis characteristics of the K-joint under cyclic loading are studied by numerical simulation. In Section 2, the numerical model of the K-joint in an actual transmission tower is established. In Section 3, the moment-rotation hysteretic curves of the K-joint are analyzed. In Section 4, the stiffness degradation of the K-joint is discussed. Then, the energy dissipation capacity of the K-joint is analyzed in Section 5. In Section 6, the failure mode of the K-joint is discussed, and finally, Section 7 concludes the study.

2. Models and Scenarios

2.1. Finite Element Model. In this paper, a K-joint of a 500 kV tower was selected as the research object, and the large-scale finite element analysis software ANSYS was used for modeling. The model is composed of a main angle steel, a gusset plate, two kinds of branch angle steel, and 10 bolts, as shown in Figure 1. Considering the calculation accuracy and efficiency, all components of the K-joint are simulated by 3D 8-node structural solid element SOLID185, the grids are divided into hexahedrons, and the grids are subdivided in the contact area of components. There are a total of 32 contact pairs in the finite element model, which can be divided into four categories, namely, the contact between the main angle steel and the gusset plate, the contact between the branch angle steel and the gusset plate, the contact between the nut and the component, the contact between the bolt head and the component, and the contact between the bolt shank and the bolt hole. Except for the bond contact mode between the bolt head and the component, the standard contact mode is adopted, and friction is considered. Since the solid element selects 8-node SOLID185, the surface-to-surface contact element adopts 3D 4-node CONTA173, which corresponds to the 3D target element TARGE170. To facilitate loading, the MPC184 element is used to establish rigid beams at the end of branch angle steel, and a rigid area is created to couple the end of branch angle steel with the end of rigid beams.

2.2. Bolt Pretension. The selected K-joints are connected by bolts, and the preload element PRETS 179 is used in ANSYS to apply the pretension force. The element can define a pretension section within any 2D or 3D structure and

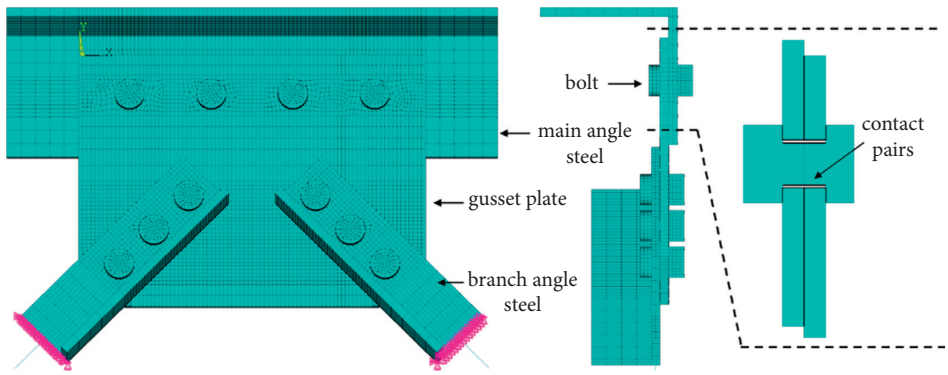

Figure 1: K-joint finite element model.

generate a preloaded area. The relationship between the bolt pretension force and initial torque is shown in the following equation:

$$P_c = \frac{T_c}{k \cdot d}, \tag{1}$$

where P_c = bolt pretension force; T_c = initial torque of bolts; $k = 0.05$, average torque coefficient of bolt connection sets, which can be determined from the relevant provisions of JGJ82-2011 Technical specification for high-strength bolt connections of steel structures [25]; and d = bolt diameter.

After the pretension force is applied, if the component around the bolt is slightly warped, it indicates that the pretension force is correctly applied.

2.3. Material Parameter. Q345 is adopted for the steel of connectors, and 6.8 grade M20 bolts are used. The friction coefficient between the connectors and between the nut and the connector is 0.3, and the eccentric distance is 50 mm. The elastic modulus of the steel is 206 GPa, the elastic modulus of the bolt is 195 GPa, and the Poisson ratio of both is 0.3. The tensile strength and yield strength of the bolts were determined according to GB/T3098.1-2010 Mechanical properties of fastener bolts, screws, and studs [26].

The constitutive relation of the components and bolts adopts the elastic-plastic model with a strengthened section, considering the Bauschinger effect, as shown in Figure 2 [27]. In Figure 2, ε_y = yield strain; $\varepsilon_{cu} = 0.02$, ultimate strain; σy = yield stress; and σ_{cu} = ultimate stress.

2.4. Simulated Conditions. In this paper, 13 groups of scenarios were simulated. The component thickness was 10 mm, and M20 bolts were used. The effects of initial torque, friction coefficient, eccentric distance, bolt hole diameter, strength of connectors, bolt spacing, and bolt grade on the hysteretic characteristics of the K-joint were studied, and the specific parameters are shown in Table 1.

The loading method is controlled by load, which is loaded synchronously along the inclined direction at the end of the rigid beam and subjected to cyclic loading of tension and compression. First, according to 25%, 50%, and 75% of the yield load, each cycle, after reaching yield, according to 10% of the ultimate load gradually increased, three times for each cycle.

The calculation method of the rotation angle and moment is illustrated in Figure 3, which are calculated by equations (2)–(5).

$$u_{\text{sum}} = \sqrt{u_x^2 + u_y^2}, \tag{2}$$

$$\sin\frac{\theta}{2} = \frac{1/2u_{\text{sum}}}{\sqrt{e^2 + w_h{}^2}}, \tag{3}$$

$$\theta = \arccos\left(1 - 2\sin^2\frac{\theta}{2}\right), \tag{4}$$

$$M = F \cdot e, \tag{5}$$

where θ = rotation angle of joint; u_x and u_y = displacement of measuring point; e = eccentric distance; and w_h = half width of gusset plate.

3. Moment-Rotation Hysteretic Curve

Since the resultant force borne by the K-joint does not pass through the centroid of the main angle steel bolt group, the moment will be generated at the centroid of the bolt group, and the gusset plate will rotate by eccentric force. In this section, the rotation angle of the gusset plate is taken as the horizontal axis and the moment is taken as the vertical axis, and the moment-rotation hysteretic curve is drawn, as shown in Figure 4.

It can be found from the figure that

(1) In the process of repeated loading, due to the existence of clearance, the bolt will slip a certain distance, which causes the hysteresis curve to be a pinched, anti-S shape.

(2) The fullness of the hysteresis curve is related to the bolt initial torque, friction coefficient, eccentricity, clearance, component strength, bolt spacing, and bolt grade. Compared with Cases 1, 2, and 3, the curve shape will be more plump when the bolt initial torque is increased, as shown in Figures 4(a)–4(c). Compared with Cases 1, 4, and 5, the curve still

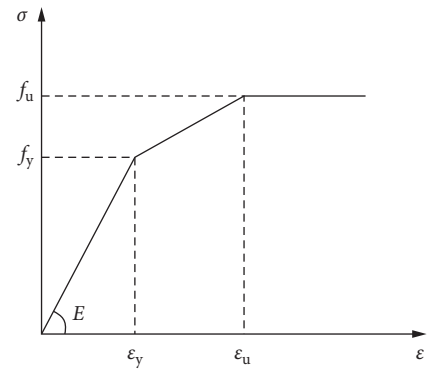

Figure 2: Constitutive relation.

Table 1: Numerical scheme.

Case no.	Initial torque (N·m)	Friction coefficient of component	Friction coefficient of nut	Eccentric distance (mm)	Bolt hole diameter (mm)	Component material	Bolt spacing (mm)	Bolt grade
Case 1	100	0.3	0.3	50	22	Q345	100	6.8
Case 2	125	0.3	0.3	50	22	Q345	100	6.8
Case 3	150	0.3	0.3	50	22	Q345	100	6.8
Case 4	100	0.2	0.3	50	22	Q345	100	6.8
Case 5	100	0.4	0.3	50	22	Q345	100	6.8
Case 6	100	0.3	0.3	50	22	Q420	100	4.8
Case 7	100	0.3	0.3	50	22	Q420	100	6.8
Case 8	100	0.3	0.3	50	22	Q420	100	8.8
Case 9	100	0.3	0.3	50	22	Q420	100	10.9
Case 10	100	0.3	0.3	50	22	Q345	80	6.8
Case 11	100	0.3	0.3	100	22	Q345	100	6.8
Case 12	100	0.3	0.3	50	20	Q345	100	6.8
Case 13	100	0.3	0.2	50	22	Q345	100	6.8

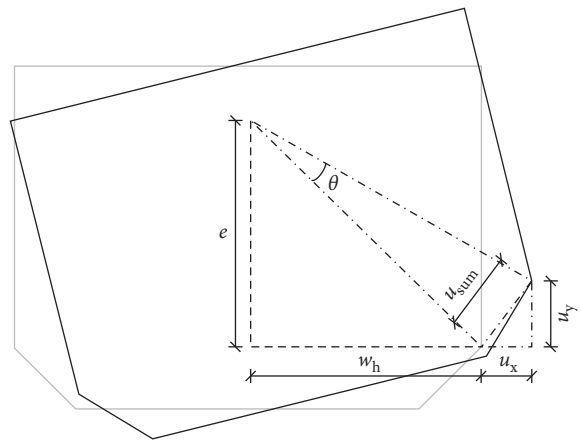

Figure 3: Diagram of rotation angle.

becomes full when the friction between members is increased, as shown in Figures 4(d) and 4(e). This is because increasing the bolt initial torque can make the members connected by bolts fit more closely and, in a sense, achieve the effect of increasing friction. Therefore, more energy is dissipated in the cycle process. As shown in Figures 4(a) and 4(g), when the member steel changes from Q345 to Q420, the ultimate bending moment increases from 21.21 kN·m to 24.75 kN·m, an increase of 16.7%. Compared with Cases 6, 7, 8, and 9, when the bolt grade is changed from 4.8 to 6.8, the ultimate bending moment increases from 16.92 kN·m to 24.75 kN·m, which increases by approximately 46.3%, and the curve is also

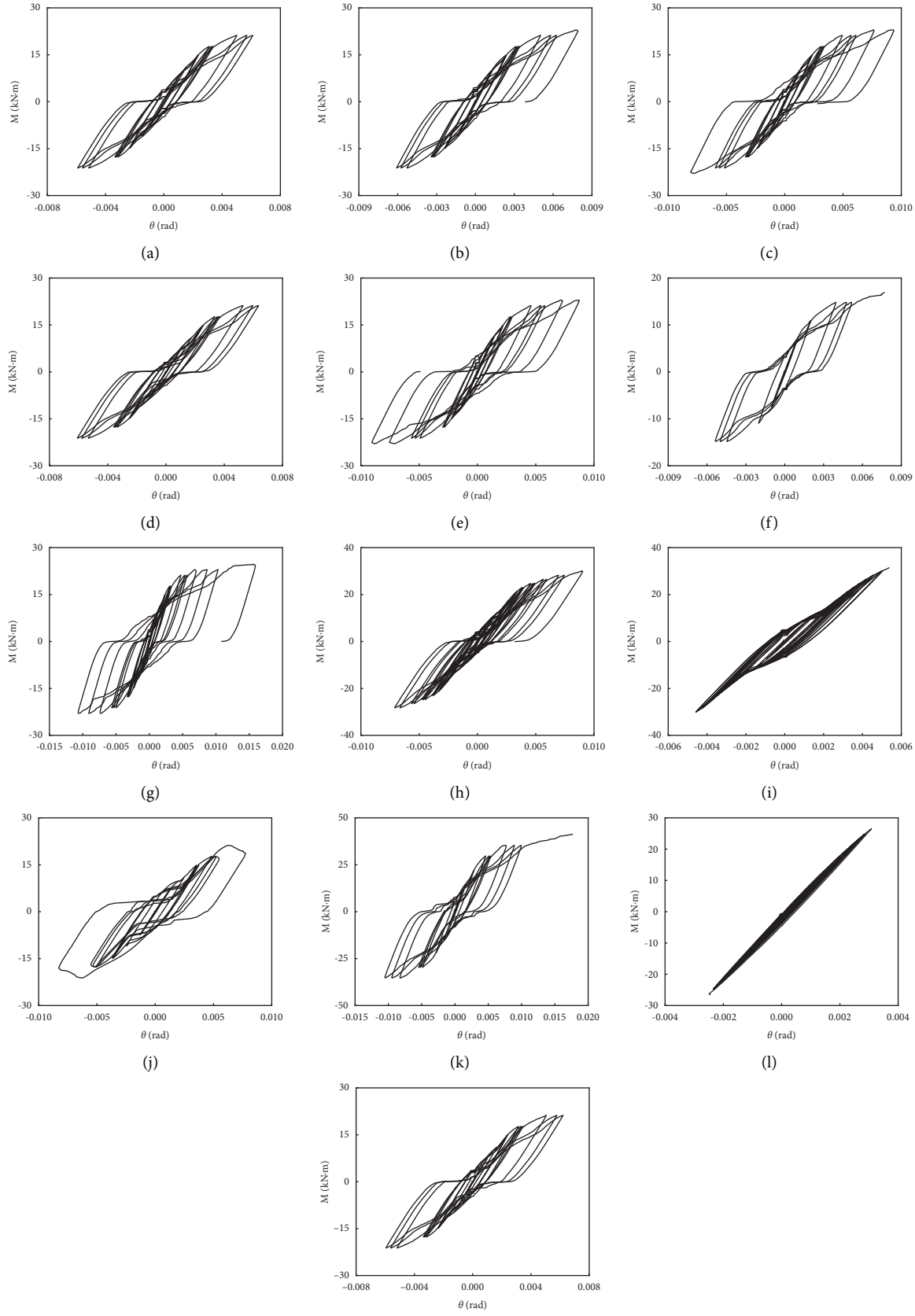

FIGURE 4: Moment-rotation hysteretic curve. (a) Case 1. (b) Case 2. (c) Case 3. (d) Case 4. (e) Case 5. (f) Case 6. (g) Case 7. (h) Case 8. (i) Case 9. (j) Case 10. (k) Case 11. (l) Case 12. (m) Case 13.

plumper, as shown in Figures 4(f) and 4(g). As the bolt grade increases from 8.8 to 10.9, the ultimate bending moment increases from 30.05 kN·m to 31.47 kN·m, which is an increase of only approximately 4.7%, but the curve is more pinched, as shown in Figures 4(h) and 4(i). The reason for these two opposite trends in the hysteresis curves is that they have different failure modes. The failures in Cases 6 and 7 are caused by bolt failure, while the failures in Cases 8 and 9 are caused by branch angle steel buckling, which will be described in detail in Section 6.

For K-joints, the rotation of the gusset plate is unfavorable to the hysteretic performance. When the spacing of the main angle steel bolt is reduced, the constraints at both ends of the gusset plate are also reduced, and the gusset plate will have a larger rotation angle under the same force, as shown in Figure 4(j). Compared with Cases 1 and 11, when the bending moment is the same, Case 11 has a larger rotation angle. According to equations (3) and (4), when the eccentric distance e increases, the rotation angle θ will also increase. As shown in Figure 4(l), when the clearance is reduced, the bolt and the bolt hole are equivalent to welding. Since the main angle steel bolt cannot slip, the rotation amplitude of the gusset plate is reduced relative to the case with slip when the bending moment is the same. Comparing Cases 1 and 13, it can be seen that the hysteresis curve has almost no change because the area of the nut is too small, and the friction coefficient cannot have decisive effects on the results.

(3) In each loading process, the slope of the curve decreases with increasing load, indicating that the connection stiffness of the joint gradually degenerates, and the residual deformation continues to accumulate and increase, which is mainly related to the yield of members and bolts and the slip of bolts.

In conclusion, the shapes of the hysteretic curves with different parameters are very different, among which the clearance, bolt grade, and member strength have the greatest influence. In addition, it is not enough to evaluate the hysteretic performance of the K-joints only by moment-rotation curve, and it needs to be judged by actual parameters.

4. Stiffness Degradation

One of the nonlinear properties of the structure beyond elasticity is the change in structural stiffness. Stiffness degradation means that under cyclic loading, when the same peak load is maintained, the displacement of the peak point increases with increasing cycle times; that is, the stiffness of the structure or component decreases with increasing repeated loading times. According to the regulations in the JGJ/T101-2015 Specification for seismic testing of buildings [28], the secant stiffness $K_{\theta i}$ under each cycle is calculated by equation (6) in this section.

$$K_{\theta i} = \frac{\left|+F_{\mathrm{i}}\right| + \left|-F_{\mathrm{i}}\right|}{\left|+X_{\mathrm{i}}\right| + \left|-X_{\mathrm{i}}\right|}, \tag{6}$$

where $+F_i$ and $-F_i$ = the load value of the ith forward and reverse peak points and $+X_i$ and $-X_i$ = the displacement value of the ith forward and reverse peak points.

Figure 5 shows the secant stiffness $K_{\theta i}$ of the moment-rotation curve for each cycle of the joint. As shown in the figure, compared with Cases 6, 7, 8, and 9, the overall stiffness of Cases 6 and 7 shows a downward trend, while the stiffness of Cases 8 and 9 decreases first, and the decline range is smaller than that of Cases 6 and 7. This is because Cases 6 and 7 use ordinary bolts, and joint failure is due to the failure of the bolts. However, high-strength bolts are used in Cases 8 and 9, and joint failure is caused by the buckling of the branch angle steel. When the branch angle steel reaches the yield strength, it becomes the main stress part. At this time, the gusset plate is less affected by the load, so the stiffness tends to be flattened.

It can also be seen from the figure that Case 12 eliminates the bolt clearance, and the entire stiffness is high. In addition, the stiffness of the K-joint with a small bolt spacing is generally low, while the stiffness degradation of other cases is generally gentle.

In addition, Table 2 shows the initial stiffness $K_{\theta o}$ of the joint under various cases, namely, the ratio of the sum of the absolute values of the load at the forward and reverse peak points under the first loading to the sum of the corresponding displacement. It can be seen from the comparison that in the elastic range, the initial stiffness of each case is similar, but reducing the clearance can significantly improve the initial stiffness of the joint.

5. Energy Dissipation Capacity

When the structure enters the plastic state, there is residual deformation and energy loss after unloading. Under cyclic loading, the area enclosed by the moment-rotation hysteresis loop represents the energy consumption. The energy dissipation coefficient C_e and equivalent viscous damping coefficient ξ_{eq} are usually used to evaluate the energy dissipation capacity of components [28]. The formulas are as follows:

$$C_e = \frac{S_{(\mathrm{ABC+CDA})}}{S_{(\mathrm{OBE+ODF})}},$$
$$\xi_{\mathrm{eq}} = \frac{1}{2\pi} \cdot \frac{S_{(\mathrm{ABC+CDA})}}{S_{(\mathrm{OBE+ODF})}}, \tag{7}$$

where $S(\mathrm{ABC} + \mathrm{CDA})$ = the area enclosed by the hysteresis curve in Figure 6 and $S(\mathrm{OBE} + \mathrm{ODF})$ = the sum of the area of triangles OBE and ODF.

The total energy consumption W_t, equivalent viscous damping coefficient ξ_{eq}, and energy dissipation coefficient C_e of the joint in the limit state are calculated, as shown in Table 3.

It can be seen from Table 3 that increasing the member strength and bolt grade and increasing the friction between components will lead to an increase in the total energy

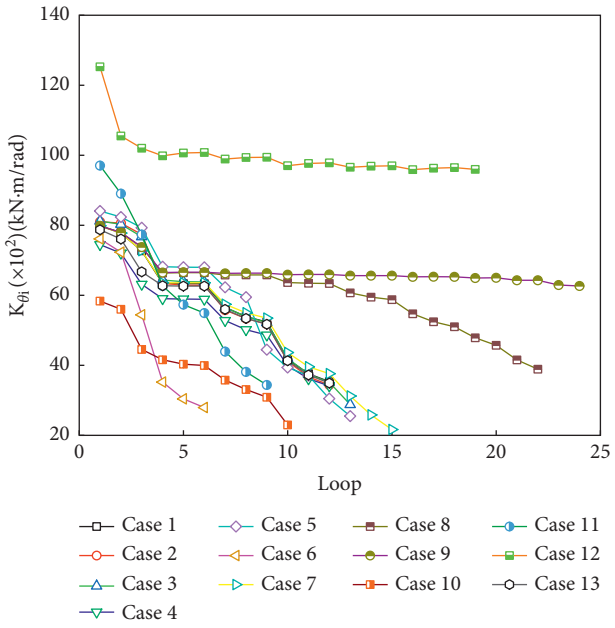

Figure 5: The stiffness degradation of moment-rotation curve.

Table 2: Initial stiffness.

Case	Initial stiffness (kN·m/rad)
1	7983.26
2	8099.91
3	8119.99
4	7447.76
5	8408.83
6	7609.41
7	7983.27
8	7984.07
9	7984.06
10	5833.96
11	9705.45
12	12524.77
13	7872.30

consumption, which indicates that these measures can improve the energy consumption of the joint. In addition, it can be seen from Table 3 that increasing the eccentricity and reducing the spacing of the main angle steel bolts will improve the energy dissipation capacity of the K-joint. However, from the hysteresis curve, increasing the eccentricity and reducing the spacing of the main angle steel bolts will cause a greater bending moment and rotation angle, which will lead to early failure of the K-joint. It cannot be simply considered that this will improve its energy dissipation capacity.

6. Failure Morphology

When the transmission tower is subjected to wind, earthquakes, and other loads, the components of the transmission tower are often subjected to repeated loads. The most unfavorable loading state for K-joints is that one side of the branch angle steel bears tension and one side of the branch angle steel bears compression. At this time, since the resultant force acting point of branch angle steel under the load does not pass through the centroid of the bolt group on the main angle steel, a moment will be generated at the centroid of the bolt group, resulting in the rotation of the gusset plate under the eccentric load, as shown in Figure 7.

6.1. Effect of Bolt Grade. To study the influence of bolt grade on the failure mode of the joint, bolts of grade 4.8, grade 6.8, grade 8.8, and grade 10.9 were used in Cases 6, 7, 8, and 9, respectively. According to the simulation results, the failure mode of Case 6 is consistent with that of Case 7, and the failure mode of Case 8 is consistent with that of Case 9. Here, Case 6 and Case 9 are selected for comparison.

Figure 8 shows the failure form of the K-joint in Case 6, that is, the bolt is damaged, and its deformation is far more than that of the other components. Figure 8(a) shows that rotation of the gusset plate occurs, and the deformation of the other components is not obvious, which is particularly clear in Figures 8(b)–8(d). From Figure 8(e), it can be seen that the main angle steel bolts have an obvious torsional trend, and the plastic strain of the main angle steel bolt is 0.08, which is much larger than 0.042 of the branch angle steel bolt, which shows that the failure of the main angle steel bolt is more serious than that of the branch angle steel bolt. The diagonal bolt shows only a shear state, and the plastic strain of the bolt shank is continuous, as shown in Figure 8(f).

Figure 9 shows the failure mode of the K-joint in Case 9; that is, the branch angle steel has obvious buckling, while the bolt deformation is not obvious. Figure 9(a) shows that the failure mode of Case 9 is obviously different from that of Case (6), and its branch angle steel shows obvious buckling. It can be seen from Figures 9(b)–9(d) that the deformation of components is greater than that of Case 6, and the deformation of branch angle steel is the most significant.

Compared with Cases 6 and 9, the plastic strain of the branch angle steel in Case 6 reached 0.0021, and that of the main angle steel bolt was 0.08, while the strain of branch angle steel in Case 9 was 0.036, and that of the bolt was 0.009, and the results were exactly the opposite. This is because in Case 6, 4.8 grade ordinary bolts were used, whose shear strength is lower than that of the component, so the bolt was cut off, resulting in joint failure. Grade 10.9 high-strength bolts were used in Case 9, whose shear strength was higher than that of the component. Under cyclic loading, joint failure was caused by buckling due to the weak strength of the inclined material.

The failure mode of the K-joint is related to the bolt grade. When the strength of the component is certain, improving the bolt grade can avoid the joint failure caused by bolt shear fracture. However, if the bolt grade is too high, the branch angle steel will buckle before the bolts are snipped, resulting in the failure of the K-joint.

6.2. Effect of Component Strength. Cases 1 and 7 are selected for analysis. Grade 6.8 ordinary bolts were used, and the components were Q345 and Q420 steel. By analyzing

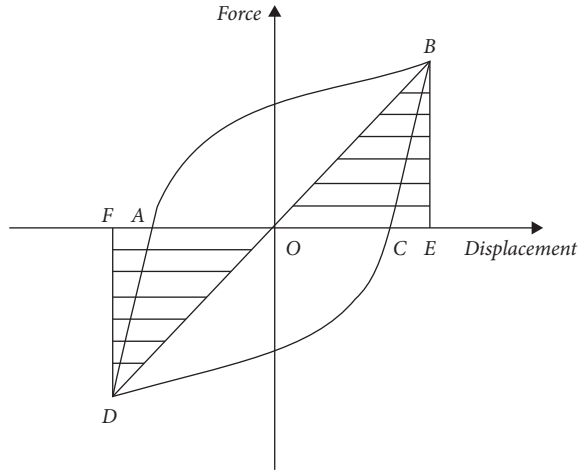

Figure 6: Calculation of the energy dissipation coefficient.

Table 3: Energy consumption index of the *K*-joint.

Case	Total energy consumption W_t (kN·m·rad)	Equivalent viscous damping coefficient ξ_{eq}	Energy dissipation coefficient C_e
1	376.109	0.108	0.676
2	488.015	0.117	0.732
3	654.693	0.152	0.953
4	370.817	0.107	0.673
5	705.373	0.151	0.948
6	225.899	0.154	0.969
7	1192.207	0.193	1.212
8	840.243	0.091	0.574
9	662.233	0.072	0.451
10	498.925	0.209	1.315
11	1197.311	0.150	0.942
12	92.665	0.027	0.168
13	376.088	0.107	0.672

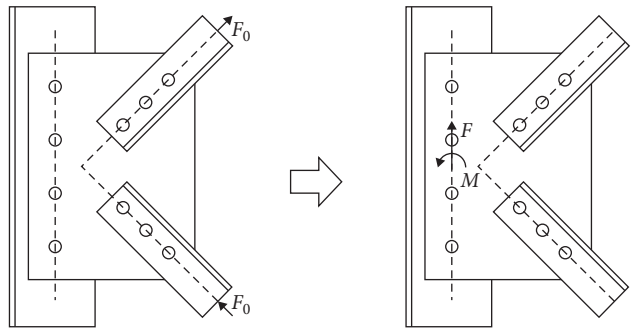

Figure 7: Mechanism of the K-joint under the most unfavorable load.

Figure 10(a), it can be seen that the joint component of Case 1 did not have large deformation, and compared with Figures 10(b) and 10(c), the bolt strain reached 0.038, and the branch angle steel strain was 0.012, indicating that the joint failure of Case 1 was the same as that of Cases 6 and 7, which was caused by bolt failure. It is obvious from Figures 10(c) and 10(f) that the deformation of branch angle steel in Case 7 is much less than that in Case 1.

Therefore, when the load is certain, improving the steel strength of the component can reduce the deformation of the component and improve the bearing performance of the joint.

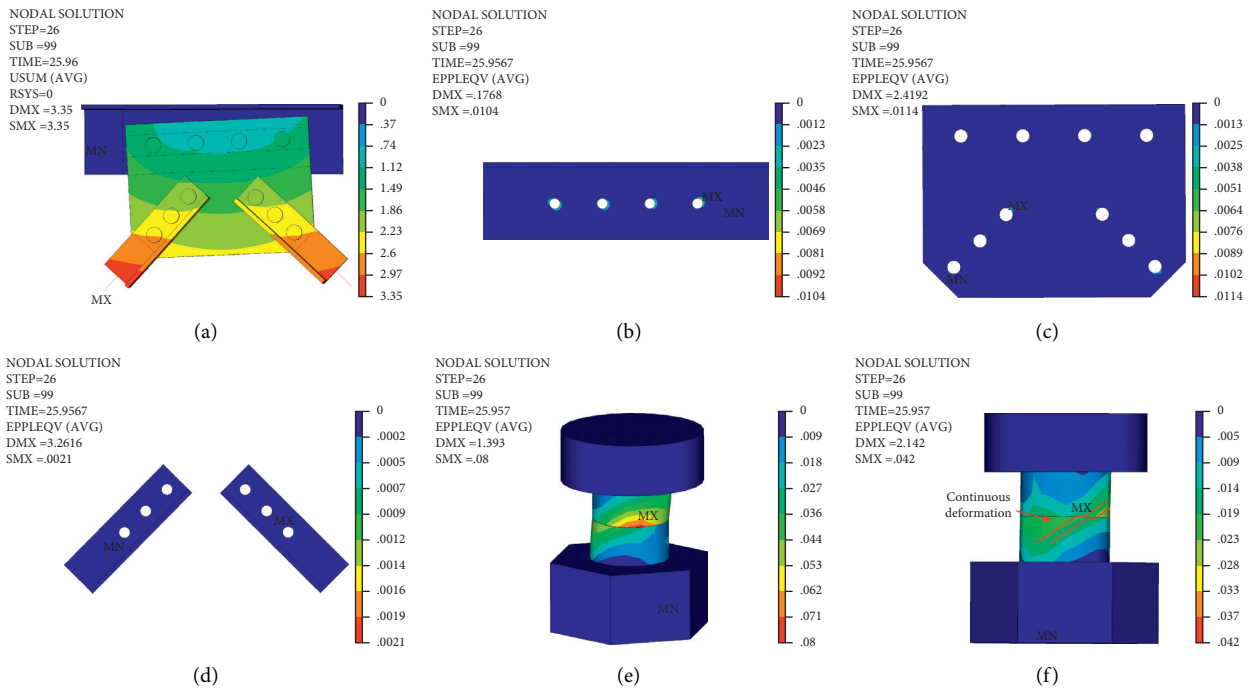

Figure 8: Simulation results for Case 6. (a) Displacement of joint. (b) Plastic strain of main angle steel. (c) Plastic strain of gusset plate. (d) Plastic strain of branch angle steel. (e) Plastic strain of bolts on main angle steel. (f) Plastic strain of bolts on branch angle steel.

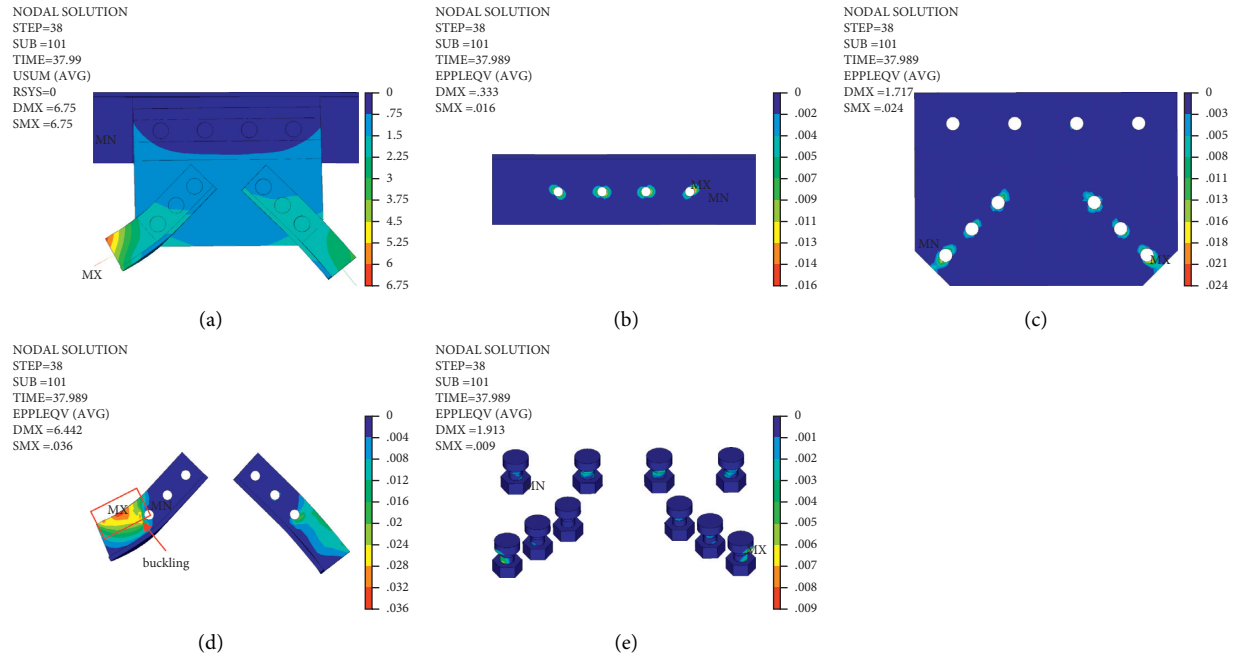

Figure 9: Simulation results for Case 9. (a) Displacement of joint. (b) Plastic strain of main angle steel. (c) Plastic strain of gusset plate. (d) Plastic strain of branch angle steel. (e) Plastic strain of bolts.

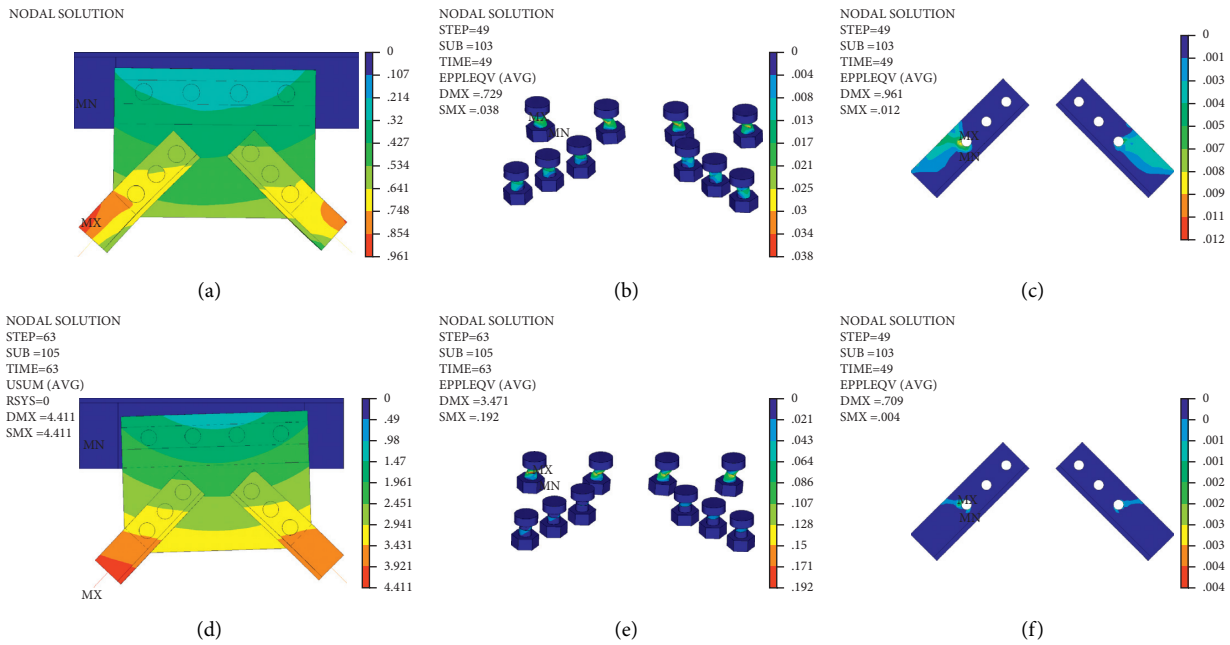

FIGURE 10: Simulation results for Cases 1 and 7. (a) Displacement of joint in Case 1. (b) Plastic strain of bolts in Case 1. (c) Plastic strain of branch angle steel in Case 1. (d) Displacement of joint in Case 7. (e) Plastic strain of bolts in Case 7. (f) Plastic strain of branch angle steel in Case 7.

7. Conclusion

In this paper, numerical simulations were performed to study the mechanical characteristics of K-joints under cyclic loading. The failure mode of the K-joints was analyzed. The mechanical properties of the K-joint were discussed from the aspects of the hysteresis curve, stiffness degradation, and energy dissipation capacity. The following conclusions were drawn:

(1) The hysteretic behavior of the K-joint is affected by the bolt initial torque, friction coefficient, eccentricity, clearance, component strength, bolt spacing, and bolt grade. Increasing the bolt initial torque, increasing the friction between components, improving the strength of components, selecting high-strength bolts, or reducing the clearance can improve the hysteretic characteristics of this type of joint.

(2) The failure mode of the *K*-joint is related to the bolt grade and component strength. When the strength of the component is certain, increasing the bolt grade can avoid the joint failure caused by bolt shear fracture. However, if the bolt grade is too high, the branch angle steel will first undergo buckle failure, resulting in K-joint failure. Therefore, special attention should be given to the selection of bolt grade and steel type.

(3) If *K*-joints have eccentricity, the main bolt group will not only bear shear force but also receive a bending moment, showing a torsional shear state. The bolt of branch angle steel only bears the shear force, so the main bolt will be damaged before the bolt of branch angle steel. In practice, the eccentricity should be reduced as much as possible. If it cannot be reduced, the grade of the main bolt should be strengthened.

(4) In the loading process, if the bolt is damaged, the secant stiffness will decrease rapidly. If the branch angle steel yields, the secant stiffness decreases gently.

(5) Increasing the eccentricity and reducing the spacing of the main angle steel bolt can improve the energy dissipation capacity of the K-joint, but it will accelerate the destruction of the K-joint.

Data Availability

No data were used to support this study.

Conflicts of Interest

The authors declare that they have no conflicts of interest.

Acknowledgments

This study was financially supported by the National Natural Science Foundation of China (grant no. 51808100) and Liaoning Provincial Natural Science Foundation of China (grant no. 2019-ZD_0004).

References

[1] C. Díaz, P. Martí, M. Victoria, and O. M. Querin, "Review on the modelling of joint behaviour in steel frames," *Journal of Constructional Steel Research*, vol. 67, no. 5, pp. 741–758, 2011.

[2] I. Faridmehr and M. Hajmohammadian Baghban, "An overview of progressive collapse behavior of steel beam-to-

column connections," *Applied Sciences*, vol. 10, no. 17, p. 6003, 2020.

[3] R. Al-fisalawi, A. Khalid, and M. Al-kamal, "Performance of semi-rigid steel connections under monotonic and cyclic loadings: a review," in *Proceedings of the Iop Conference Series: materials Science and Engineering*, no. 1, p. 1067, Prague Czech Republic, September 2021.

[4] C. Zhu, K. J. R. Rasmussen, S. Yan, and H. Zhang, "Experimental full-range behavior assessment of bolted moment end-plate connections," *Journal of Structural Engineering*, vol. 145, no. 8, pp. 1–12, 2019.

[5] G. Zhou, Y. An, D. Li, and J. Ou, "Analytical model of moment-rotation relation for steel beam to CFST column connections with bidirectional bolts," *Engineering Structures*, vol. 196, no. 2, Article ID 109374, 2019.

[6] I. Faridmehr, M. M. Tahir, M. H. Osman, and M. Azimi, "Cyclic behaviour of fully-rigid and semi-rigid steel beam-to-column connections," *International Journal of Steel Structures*, vol. 20, no. 2, pp. 365–385, 2020.

[7] Y. Shao, S. He, and D. Yang, "Prediction on static strength for CHS tubular K-joints at elevated temperature," *Ksce Journal of Civil Engineering*, vol. 21, no. 3, pp. 900–911, 2017.

[8] N. Azari Dodaran, H. Ahmadi, and M. A. Lotfollahi-yaghin, "Parametric study on structural behavior of tubular K-joints under axial loading at fire-induced elevated temperatures," *Thin-Walled Structures*, vol. 130, pp. 467–486, 2018.

[9] R. Feng, C. Tang, Z. Chen, K. Roy, B. Chen, and J. B. M. Lim, "A numerical study and proposed design rules for stress concentration factors of stainless steel hybrid tubular k-joints," *Engineering Structures*, vol. 233, no. 52, Article ID 111916, 2021.

[10] R. Feng, J. Lin, and X. Mou, "Experiments on hybrid tubular K-joints with circular braces and square chord in stainless steel," *Engineering Structures*, vol. 190, pp. 52–65, 2019.

[11] Y. Lu, K. Liu, Z. Wange, and W. Tang, "Dynamic behavior of scaled tubular k-joints subjected to impact loads," *Marine Structures*, vol. 69, Article ID 102685, 2020.

[12] F. Li, H.-z. Deng, and X.-y. Hu, "Resistance of gusset-tube DK-joints stiffened by 1/2 annular plates in transmission towers," *Journal of Constructional Steel Research*, vol. 159, pp. 560–573, 2019.

[13] F. Li, H. Deng, and X. Hu, "Design resistance of longitudinal gusset-tube k-joints with 1/4 annular plates in transmission towers," *Thin-Walled Structures*, vol. 144, Article ID 106271, 2019.

[14] W. Q. Jiang, Z. Q. Wang, G. Mcclure, G. L. Wang, and J. D. Geng, "Accurate modeling of joint effects in lattice transmission towers," *Engineering Structures*, vol. 33, no. 5, pp. 1817–1827, 2011.

[15] W. Jiang, Y. Liu, S. Chan, and Z. Q. Wang, "Direct analysis of an ultrahigh-voltage lattice transmission tower considering joint effects," *Journal of Structural Engineering*, vol. 143, no. 5, Article ID 4017009, 2017.

[16] F. Yang, B. Zhu, and H. Xing, "THE slip characteristics and parametric study of bolted connections for transmission towers," *Engineering Mechanics*, vol. 34, no. 10, pp. 116–127, 2017, in Chinese.

[17] L. An, J. Wu, and W. Jiang, "Experimental and numerical study of the axial stiffness of bolted joints in steel lattice transmission tower legs," *Engineering Structures*, vol. 187, pp. 490–503, 2019.

[18] Y.-d. Gan, H.-z. Deng, and C. Li, "Simplified joint-slippage model of bolted joint in lattice transmission tower," *Structure*, vol. 32, pp. 1192–1206, 2021.

[19] N. Zhao, Z. Li, and H. Liu, "Calculation model of initial stiffness of angle steel tower k-joints," *Engineering Mechanics*, vol. 31, no. 4, pp. 93–101, 2014, in Chinese.

[20] F. Yang, B. Zhu and Z. Li, Numerical analysis and full-scale experiment on k-joint deformations in the crank arms of lattice transmission towers," *The Structural Design of Tall and Special Buildings*, vol. 27, no. 5, p. 1448, 2018.

[21] J. Li, G. Mcclure, and S. Wang, "Ensuring the structural safety of overhead transmission lines by design," *Journal of Aerospace Engineering*, vol. 34, no. 3, Article ID 4021010, 2021.

[22] M. Saleem and M. Saleem, "Cyclic shear-lag model of steel bolt for concrete subjected to impact loading," *Journal of Materials in Civil Engineering*, vol. 30, no. 3, Article ID 04018023, 2018.

[23] J. Li, B. Wang, J. Sun, and S. H. Wang, "Numerical simulation study on hysteresis characteristics of transmission tower bolt joints," *Journal of Northeastern University*, vol. 41, no. 11, pp. 1633–1639, 2020, in Chinese.

[24] L. Ma and P. Bocchini, "Hysteretic model of single-bolted angle connections for lattice steel towers," *Journal of Engineering Mechanics*, vol. 145, no. 8, Article ID 04019052, 2019.

[25] Jgj82-2011, *Technical Specification for High Strength Bolt Connections of Steel structures*, China Architecture & Building Press, Beijing, China, 2011, in Chinese.

[26] Gb/T3098 1-2010, *Mechanical Properties of Fasteners-Bolts, Screws and Studs*, Standards Press of China, Beijing, China, 2010, in Chinese.

[27] J. Li, H. Li, and X. Fu, "Stability and dynamic analyses of transmission tower-line systems subjected to conductor breaking," *International Journal of Structural Stability and Dynamics*, vol. 17, no. 6, Article ID 1771013, 2017.

[28] Jgj/T101-2015, *Specification for Seismic Test of Buildings*, China Architecture & Building Press, Beijing, China, 2015, in Chinese.